# Early stages of spinodal decomposition in superfluid $^3$He-$^4$He mixtures

P. C. Hohenberg
*Bell Laboratories, Murray Hill, New Jersey 07974*

David R. Nelson
*Department of Physics, Harvard University, Cambridge, Massachusetts 02138*
(Received 21 May 1979)

A generalization of the linearized analysis of Cahn, Hilliard, and Cook is applied to a simple model of phase separation dynamics in $^3$He-$^4$He mixtures at early times. An instability region is found in which the structure function for concentration fluctuations exhibits maximum growth at a nonzero wave vector. The coupling of concentration fluctuations to the superfluid second-sound mode produces an additional "flickering" component in the scattering. Equilibrium experimental data from both sides of the coexistence curve are used to estimate the size of these effects. The instability region is found to be quite asymmetrically placed inside the two-phase region.

## I. INTRODUCTION

There has been considerable interest recently in the dynamics of phase separation, particularly in alloys,[1] and in binary fluid mixtures.[2] Rapid quenches into the two-phase region of such substances [Fig. 1(a)] are followed by a coarsening into two phases. When the order parameter is conserved by the dynamics, as is the case for the examples cited above, one expects unstable order-parameter fluctuations at a preferred nonzero wave vector. Indeed, light scattering experiments on binary mixtures[2] reveal a striking ring-shaped intensity pattern during the initial stage of the separation. Such behavior is expected within the unstable "spinodal" region shown in Fig. 1(a); outside of this region, separation requires thermal activation and proceeds via a nucleation mechanism.[1]

Although a complete description of the separation into two phases is a formidable problem,[3] the initial coarsening can be qualitatively understood using an approach due to Cahn,[4] Hilliard,[5] and Cook.[6] To treat binary alloys at a fixed mean concentration, for example, one first writes down a phenomenological model of the dynamics of the conserved order parameter $c(\vec{x},t)$, namely,

$$\frac{\partial c}{\partial t} = \lambda \nabla^2 \frac{\delta F}{\delta c} + \eta \ , \tag{1.1}$$

where

$$F = \int d^3x \left[\tfrac{1}{2} r c^2 + \tfrac{1}{2} (\vec{\nabla} c)^2 + u c^4\right] \tag{1.2}$$

and $\eta(\vec{x},t)$ is a Gaussian noise source with correlations

$$\langle \eta(\vec{x},t)\eta(\vec{x}',t')\rangle = -2k_B T \lambda \nabla^2 \times \delta(\vec{x}-\vec{x}')\delta(t-t') \ , \tag{1.3}$$

and zero mean. Here, $c(x,t)$ represents the deviation of the concentration from its critical value.

Let us suppose the system is quenched from an initial state in the one-phase region to a point in the two-phase region, represented by a temperature $\bar{r} < 0$, and a concentration $\bar{c}$ [see Fig. 1(a)]. The basic approximation made in Refs. 4–6 is to *linearize* the diffusion equation (1.1) about the state $(\bar{r},\bar{c})$ immediately after the quench,

$$\frac{\partial}{\partial t} c(\vec{x},t) = \lambda \nabla^2 (\bar{r} - \nabla^2 + 12 u \bar{c}^2)\, c(\vec{x},t) + \eta(\vec{x},t) \ . \tag{1.4}$$

A straightforward calculation[1] then shows that the Fourier transformed equal-time correlation function is

$$S(k,t) \equiv \langle c_k(t) c_{-k}(t)\rangle = \left[S(k,0) - \frac{\lambda}{D}\right] \exp(-2Dk^2 t) + \frac{\lambda}{D} \ , \tag{1.5}$$

where $D$ is a wave-vector-dependent diffusion constant

$$D = D(k) = \lambda[-|\bar{r}|(1 - 3\bar{c}^2/c_s^2) + k^2] \equiv \lambda \chi^{-1}(k) \ , \tag{1.6}$$

and $c_s^2 \equiv |\bar{r}|/4u$ describes the coexistence curve. The quantity $\chi^{-1}(k)$ is a wave-vector-dependent concentration susceptibility continued into the two-phase region, and $S(k,0)$ describes the correlations just before the quench. It follows from Eq. (1.6) that for

$$\bar{c}^2 < \tfrac{1}{3} c_s^2 \equiv c_\sigma^2 \ , \tag{1.7a}$$

the correlation function $S(k,t)$ will grow in time over a range of $k$ with a maximum growth rate at

$$k_m = [\tfrac{1}{2}|\bar{r}|(1 - 3\bar{c}^2/c_s^2)]^{1/2} \ . \tag{1.7b}$$

 

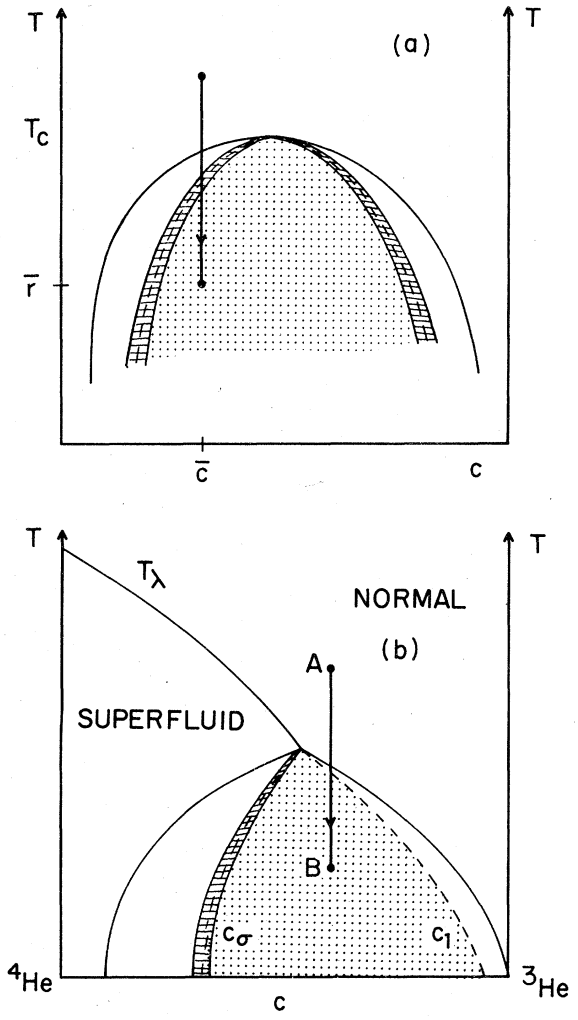


FIG. 1. Schematic temperature-concentration phase diagram for a binary mixture or alloy. A quench in temperature is indicated by the vertical arrow, and concentration fluctuations are unstable following such a quench in the shaded ("spinodal") region. Two fuzzy "spinodal" lines bound the instability region. (b) Temperature-concentration phase diagram for $^3$He-$^4$He mixtures. A quench from the normal phase is indicated by the line segment $AB$; quenches from the superfluid phase are also possible. The asymmetric shaded region of unstable concentration fluctuations is now bounded by a fuzzy spinodal line $c_\sigma$ on the left, and a somewhat sharper spinodal line $c_1$ on the right.

It should be mentioned that the existence of a sharp "spinodal line" $\bar{c}^2 = c_\sigma^2$, separating unstable and metastable regions, as well as the vanishing of $k_m$ on this line, are artifacts of the linearization.

$^3$He-$^4$He mixtures also phase separate, below a tricritical point which terminates a $\lambda$ line of continuous superfluid transitions [Fig. 1(b)]. The separation is now into a $^4$He-rich superfluid phase and a $^3$He-rich normal phase,[7] and one expects that the superfluid degrees of freedom will participate in any spinodal decomposition. The equilibrium properties of mixtures along the coexistence curve have already been studied with light scattering.[8,9] Experiments analogous to those of Ref. 2, capable of studying $^3$He-$^4$He mixture spinodal instabilities, are also feasible.[10]

With such experiments in mind, we have applied the Cahn-Hilliard-Cook analysis to a phenomenological model of the dynamics of superfluid mixtures, studied by Siggia and Nelson.[11] The model reproduces the superfluid hydrodynamics of Khalatnikov[12] and Griffin[13] near equilibrium, and it can be used to study phase separation dynamics as well. In contrast to binary alloys, concentration fluctuations in superfluid mixtures are coupled to fluctuations in two other conserved quantities, the superfluid velocity and a local entropy variable. The magnitude of the order parameter, on the other hand, is not conserved, and we have assumed that it relaxes rapidly to a value determined by the local concentration and temperature.

As illustrated in Fig. 1(b), we find an asymmetric spinodal region where concentration fluctuations are inherently unstable. Instead of Eq. (1.5), concentration fluctuations take the form

$$S(k,t) \equiv \langle c_k(t) c_{-k}(t) \rangle = a_1 e^{-2\bar{D}_0 k^2 t} + a_2 e^{-(\bar{D}_0+\bar{D}_2)k^2 t} \cos \bar{u}_2 k t + a_3 e^{-2\bar{D}_2 k^2 t} \cos 2\bar{u}_2 k t + a_0 \ , \quad (1.8)$$

where $c_k(t)$ is the spatial Fourier transform of the $^3$He concentration. The coefficients $a_i$ are time independent, but depend in a complicated way on the hydrodynamic parameters and the initial conditions. The diffusion constant $\bar{D}_0(k)$ is negative over a range of wave vectors, in analogy to Eq. (1.6). However, $\bar{u}_2(k)$ and $\bar{D}_2(k)$, which are nonequilibrium versions of the second-sound velocity and damping rate, are typically positive, at least near the tricritical point. Thus, the first term of Eq. (1.8) grows, while the oscillating third term dies out in time. The second term, which also oscillates, grows or shrinks depending on the sign of $\bar{D}_0 + \bar{D}_2$. Unfortunately, we find that $\bar{D}_0 + \bar{D}_2$ is typically positive near the tricritical point, so the oscillating components of Eq. (1.8) may be difficult to detect experimentally. We also find a region at lower temperatures where the second-sound mode becomes unstable, but the validity of our model is more questionable there. Estimates of the damping rates and velocity in Eq. (1.8) can be found in Sec. III B.

Spinodal lines dividing instability and nucleation-activated phase separation are usually rather fuzzy,[1] as indicated in Fig. 1(a). Although this is true of the "superfluid" spinodal line $c_\sigma$ in Fig. 1(b), the "normal" spinodal line $c_1$ is much more precise, at least in

the mean-field approximation. Whereas the inverse concentration susceptibility (continued into the two-phase region) passes continuously through zero on the line $c_\sigma$, it turns out to change sign discontinuously along the line $c_1$.

These results apply only to the early stages of phase separation in superfluid $^3$He-$^4$He mixtures when linearization of the equations of motion might be valid. We have not attempted to study later stages, nor have we examined in detail critical fluctuation effects which occur in the dynamics as one approaches the tricritical point.[11]

In Sec. II, the model is defined, and its equilibrium properties are discussed. Phase separation dynamics is treated in Sec. III. A number of detailed computations are contained in Appendices A–C.

## II. MODEL OF $^3$He-$^4$He MIXTURES

### A. Statics

We shall use a version of the model considered by Siggia and Nelson[11] in a study of critical dynamics near equilibrium. The statistical weight associated with a particular configuration of the fluctuating concentration $c(\vec{x})$ and the complex superfluid order parameter $\psi(\vec{x})$ is taken to be proportional to

$$\exp\left[-(1/v_0)\int d^3x\, \mathcal{F}(\psi,c)\right] ,$$

where $v_0$ is the volume per particle, and

$$\mathcal{F}=\tfrac{1}{2}|\vec{\nabla}\psi|^2+\tfrac{1}{2}r|\psi|^2+u|\psi|^4+v|\psi|^6 +\tfrac{1}{2}l_0^2|\nabla c|^2+\tfrac{1}{2}\chi_n^{-1}c^2+\gamma c|\psi|^2-\Delta c \quad . \quad (2.1)$$

The quantity $c(x)$ can be thought of as the local $^3$He concentration measured from some reference value, and $l_0$ is a length. For simplicity we take $r$, $u$, $v$, $\gamma$, and $\chi_n$ to depend only on the temperature $T$; the chemical potential $\Delta=\mu_3-\mu_4+\Delta_0$ enters the last term only ($\Delta_0$ is a constant). In Ref. 11, the term linear in $c$ was eliminated by shifting the reference $^3$He concentration, and $r$, $u$, $\gamma$, etc., were taken to be unspecified analytic functions of $T$ and $\Delta$. An additional fluctuating "entropy" variable was included in $\mathcal{F}$ because of the role it plays in the dynamics, but we shall suppress it in this subsection, since it does not affect the statics in the present model.

The mean-field approximation to the free-energy density $F(T,\Delta)$ is obtained by minimizing Eq. (2.1) over $c$ and $\psi$, for fixed $T$ and $\Delta$,

$$F(T,\Delta)=\min_{|\psi|,c}\left(\tfrac{1}{2}r|\psi|^2+u|\psi|^4+v|\psi|^6 +\tfrac{1}{2}\chi_n^{-1}c^2+\gamma c|\psi|^2-\Delta c\right) \quad . \quad (2.2)$$

We have omitted the gradient terms since they vanish in mean-field theory for a uniform system, and have included a factor $(k_BT)^{-1}$ in the definition of $F(T,\Delta)$; we also assume that $v$ and $\chi_n^{-1}$ are positive for stability. The phase diagram follows simply by first minimizing Eq. (2.2) over $c$ with $\psi$ fixed, to obtain

$$F(T,\Delta)=\min_{|\psi|}\left(\tfrac{1}{2}\tilde{r}|\psi|^2+\tilde{u}|\psi|^4+v|\psi|^6\right)+\tfrac{1}{2}\chi_n\Delta^2 \quad , \quad (2.3a)$$

where

$$\tilde{r}=r+2\gamma\Delta\chi_n \quad , \quad (2.3b)$$

$$\tilde{u}=u-\tfrac{1}{2}\chi_n\gamma^2 \quad , \quad (2.3c)$$

and we have substituted

$$c=\chi_n(\Delta-\gamma|\psi|^2)\equiv c_n-\gamma\chi_n|\psi|^2 \quad (2.4)$$

into Eq. (2.2). The phase diagram and thermodynamic functions near the tricritical point are now given by the well-known results of minimizing Eq. (2.3a) to obtain $|\psi|^2(T,\Delta)$.[14] For $\tilde{u}>0$, there is a line of second-order transitions at $\tilde{r}\equiv 0$, i.e., at $r=r_c(\Delta)=-2\gamma\Delta\chi_n$. For negative $\tilde{u}$, there is a line of first-order transitions at $\tilde{r}=\tilde{u}^2/2v$, with a tricritical point at $\tilde{r}=0$, $\tilde{u}=0$. The different phases and phase boundaries in the $T-\Delta$ plane are shown in Fig. 2. The value of $|\psi|$ on the superfluid side of the first-order line is

$$|\psi|^2\equiv\psi_s^2=|\tilde{u}|/2v \quad , \quad (2.5)$$

while the associated jump in concentration follows from inserting this into Eq. (2.4),

$$c_n-c_s=\gamma\chi_n|\tilde{u}|/2v \quad . \quad (2.6)$$

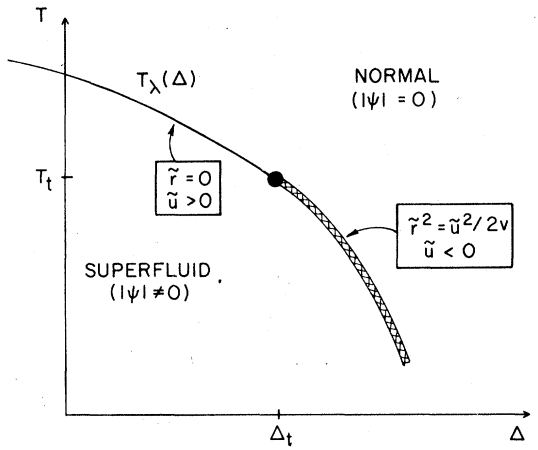


FIG. 2. Temperature–chemical-potential phase diagram for $^3$He-$^4$He mixtures. The λ line defined by the condition $\tilde{r}=0$, $\tilde{u}>0$ terminates at the tricritical point $(T_t,\Delta_t)$. The heavy line of first-order transitions below $T_t$ has an equation $\tilde{r}=\tilde{u}^2/2v, \tilde{u}<0$.

It is tedious but straightforward to verify that the concentration susceptibility obtained from Eq. (2.3) is

$$\chi \equiv \left(\frac{\partial^2 F}{\partial \Delta^2}\right)_T = \chi_n \left(\frac{u+3v|\psi|^2}{\tilde{u}+3v|\psi|^2}\right) , \tag{2.7a}$$

when $|\psi| \neq 0$, and

$$\chi = \chi_n \tag{2.7b}$$

otherwise. On the superfluid side of the coexistence curve, Eqs. (2.7a) and (2.5) reduce to

$$\chi \equiv \chi_s = \chi_n \left[1 + 2\left(\frac{u+|\tilde{u}|}{|\tilde{u}|}\right)\right] . \tag{2.8}$$

Note that $\chi_s$ diverges like $|\tilde{u}|^{-1}$ as the tricritical point is approached, but that the susceptibility remains finite ( and equal to $\chi_n$) on the normal branch of the existence curve. This artifact of the mean-field approximation will be discussed further in Sec. III.

### B. Dynamics

The dynamics of $\psi(x,t)$ and $c(x,t)$ is defined by the equations[11]

$$\frac{\partial \psi(x,t)}{\partial t} = -2\Gamma \frac{\delta W}{\delta \psi^*} - ig_1 \psi \frac{\delta W}{\delta q} - ig_2 \psi \frac{\delta W}{\delta c} + \eta_\psi(x,t) , \tag{2.9a}$$

$$\frac{\partial c(x,t)}{\partial t} = 2g_2 \mathrm{Im}\left(\psi^* \frac{\delta W}{\delta \psi^*}\right) + L\nabla^2 \frac{\delta W}{\delta q} + \lambda \nabla^2 \frac{\delta W}{\delta c} + \eta_c(x,t) , \tag{2.9b}$$

$$\frac{\partial q(x,t)}{\partial t} = 2g_1 \mathrm{Im}\left(\psi^* \frac{\delta W}{\delta \psi^*}\right) + K\Delta^2 \frac{\delta W}{\delta q} + L\nabla^2 \frac{\delta W}{\delta c} + \eta_q(x,t) , \tag{2.9c}$$

with

$$W \equiv \frac{1}{v_0} \int d^3x \left(\mathfrak{F} + \tfrac{1}{2} C^{-1} q^2\right) \tag{2.10}$$

and the $\eta_i$ are Gaussian white noise sources with zero mean and correlations

$$\langle \eta_\psi(1) \eta_\psi^*(1') \rangle = 4\mathrm{Re}\Gamma \delta(1-1') , \tag{2.11a}$$

$$\langle \eta_c(1) \eta_c(1') \rangle = 2\lambda \nabla^2 \delta(1-1') , \tag{2.11b}$$

$$\langle \eta_q(1) \eta_q(1') \rangle = -2K\nabla^2 \delta(1-1') , \tag{2.11c}$$

$$\langle \eta_c(1) \eta_q(1') \rangle = -2L\nabla^2 \delta(1-1') , \tag{2.11d}$$

and all other cross-correlations equal to zero. The variable $q$ represents the "entropy", which couples to the superfluid order parameter in pure $^4$He to make second sound.[11] Note that we have not inserted a term $\gamma_2 q|\psi|^2$ in the free energy $W$, so that our model corresponds to the "symmetric" model of superfluid helium,[15] with no singularity in the specific heat $C$ at the phase transition. Since the specific heat does not diverge at the tricritical point, this should be an adequate approximation. The constants, $\Gamma$, $g_1$, $g_2$, $K$, $L$, and $\lambda$ are dynamic parameters of the model, whose physical significance will be discussed below.

If we linearize the equations about same point in either the one-phase or two-phase regions, we find that $|\psi|$ at long wavelengths relaxes rapidly to a value given by minimizing Eq. (2.2) with fixed concentration. Near equilibrium in the superfluid phase, the Fourier transformed variables $q$, $c$, and the phase $\theta$ of $\psi$,

$$\psi(x,t) = |\psi(x,t)| e^{i\theta(x,t)} , \tag{2.12}$$

now satisfy the hydrodynamic equations

$$\frac{\partial \theta_k}{\partial t} = -\Gamma k^2 \theta_k + g_1 C^{-1} q_k + g_2 \chi^{-1} c_k + \eta_\theta , \tag{2.13a}$$

$$\frac{\partial q_k}{\partial t} = -g_1 |\psi|^2 k^2 \theta_k - Kk^2 C^{-1} q_k - Lk^2 \chi^{-1} c_k + \eta_q , \tag{2.13b}$$

$$\frac{\partial c_k}{\partial t} = -g_2 |\psi|^2 k^2 \theta_k - Lk^2 C^{-1} q_k - \lambda k^2 \chi^{-1} c_k + \eta_c , \tag{2.13c}$$

where

$$\langle \eta_\theta(k) \eta_\theta^*(k') \rangle = 2\Gamma k^2 \delta(k-k') . \tag{2.13d}$$

Equations (2.13) lead to a diffusion mode and two coupled second-sound modes.[11] In the normal phase, $|\psi|$ vanishes, and one is left with two coupled diffusion modes for $q$ and $c$. First-sound excitations, which occur at much higher frequencies, are neglected in this model.

## III. SPINODAL DECOMPOSITION

Consider a $^3$He-$^4$He mixture, initially in equilibrium in the normal or superfluid one-phase regions, which is suddenly quenched into the two-phase region by lowering the temperature. Figure 1(b) shows such a quench, from the normal phase. Slow thermal diffusion times may make rapid temperature quenches difficult in practice; one alternative is to enter the two-phase region by abruptly changing the pressure.[10] Although it is easier conceptually to think

of a temperature quench, our results should apply to pressure quenches as well.

Figure 3(a) shows the three-dimensional coexistence *volume* necessary to describe phase separating mixtures. A quench produces an initial unstable or metastable state within this volume, and one then wants to follow the dynamics as the system separates into the two coexisting equilibria indicated by the heavy lines.

A first step toward understanding this decomposition is to determine spinodal lines in the $T-c$ plane within which the nonequilibrium concentration susceptibility is negative. This is done in Sec. III A. As we shall see, a negative susceptibility is associated with anomalous concentration fluctuations, just as for the simple example discussed in the Introduction.

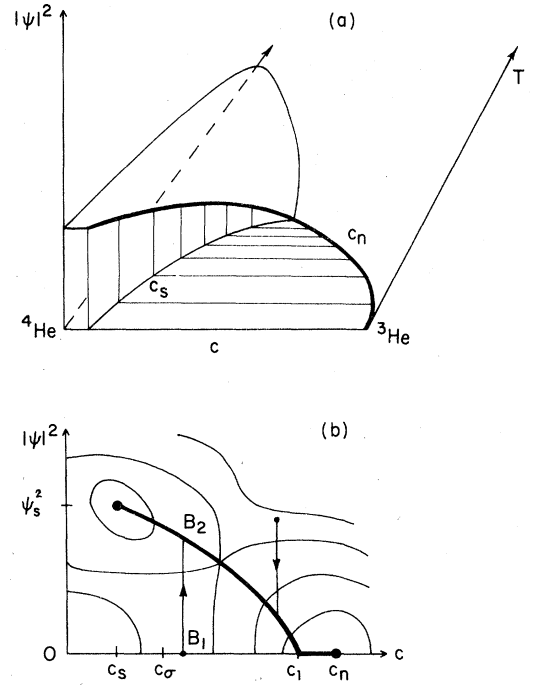


FIG. 3. (a) Squared superfluid order parameter $|\psi|^2$ as a function of temperature and concentration. At equilibrium, a three-dimensional coexistence volume describes a $^4$He-rich phase with $|\psi|^2=\psi_s^2(T)$, $c=c_s(T)$, coexisting with a $^3$He-rich phase with $|\psi|^2=0$, $c=c_n(T)$. A system quenched into this coexistence volume will ultimately decay to a two-phase equilibrium of phases given by the two heavy lines. (b) Cross section of the coexistence volume at fixed temperature. Contours of the thermodynamic potential $F(|\psi|,c)$ continued into the two-phase region are shown. Degenerate minima occur at $(\psi_s^2,c_s)$ and $(0,c_n)$, with a saddle point in between. Because $|\psi|$ is not conserved, it relaxes rapidly to the heavy line connecting the minima, while the concentration remains fixed. Two such rapid relaxations, representing quenches from the normal and superfluid phases, are indicated by vertical arrows.

### A. Constrained superfluid order parameter and concentration susceptibility

According to Eq. (2.9a), the superfluid order parameter is not conserved, and obeys instead an equation of the form

$$\frac{\partial\psi}{\partial t}=-2\Gamma\frac{\delta W}{\delta\psi^*}+\cdots+\eta_\psi\ , \tag{3.1}$$

where the dots represent mode-coupling terms. The fields $c$ and $q$, on the other hand, are conserved, and they couple to the phase of $\psi$. Because of the absence of $\nabla^2$ in Eq. (3.1), we shall assume that immediately after the quench, the magnitude $|\psi|$ of the order parameter relaxes rapidly to a *constrained* value $\bar{\psi}$, determined by the initial values of the conserved quantity $c$ and the temperature. It follows that after the quench we may consider the considerably simpler problem of dynamics on a *surface* within the coexistence volume of Fig. 3(a).

The subsequent phase separation then proceeds more slowly since it is limited by hydrodynamic processes. The initial stages can be discussed using the linearized equations of motion, with $|\psi|$ adjusted to its constrained value $\bar{\psi}$. Since by Eq. (2.7a) the concentration susceptibility $\chi$ depends on $|\psi|$, it will also assume a constrained value $\chi\equiv\bar{\chi}$, which determines the dynamics of concentration fluctuations.

Neglecting the gradient terms in Eq. (2.1), and ignoring thermal fluctuations, one finds from Eq. (3.1) that the relaxation of the *magnitude* of $\psi$ is determined by

$$\frac{\partial|\psi|}{\partial t}=-\Gamma\frac{\delta\mathcal{F}}{\delta|\psi|}=-2\Gamma|\psi|\gamma[c-\bar{c}(|\psi|)]\ , \tag{3.2a}$$

where

$$\bar{c}(|\psi|)=-\left[\frac{r}{2\gamma}+\frac{2u}{\gamma}|\psi|^2+\frac{3v}{\gamma}|\psi|^4\right]\ . \tag{3.2b}$$

Figure 3(b) shows a cross section of the coexistence volume at fixed temperature. Contours of constant free-energy density $\mathcal{F}(\psi,c)$ are also shown. Immediately after a quench, $|\psi|$ is rapidly driven by Eq. (3.2) either to zero or to the solution $\bar{\psi}$ of

$$c=\bar{c}(\bar{\psi})\ . \tag{3.3}$$

We assume that the conserved concentration variable remains fixed during this initial relaxation. It follows from Eq. (3.2) that the solution $|\psi|=0$ is stable only for

$$c_1<c<c_n\ , \tag{3.4a}$$

where

$$c_1=-r/2\gamma\ , \tag{3.4b}$$

and the solution (3.3) is stable for

$$c_s<c<c_1\ . \tag{3.4c}$$

The locus of stable constrained values to which $|\psi|$ relaxes is shown by the heavy line in Fig. 3(b). We shall relate $c_1$ to measurable quantities below.

Let us illustrate the foregoing discussion with an example. Consider the quench corresponding to the segment $AB$ of Fig. 1(b). Immediately after the quench, one has $|\psi|=0$ and $c=c_i$, which we represent as the point $B_1$ in the $(|\psi|,c)$ plane [Fig. 3(b)]. Noise fluctuations neglected in the equation of motion (3.2a) will force $|\psi|$ off this unstable extremum, and allow the rapid relaxation represented by the arrow $B_1B_2$ to the point $B_2$ on the line $|\psi|=\bar{\psi}(c)$. In the $(T,c)$ plane of Fig. 1(b), the system has remained at $B$, since the concentration and temperature have not changed.

Associated with the locus $\bar{\psi}(c)$ is a "constrained susceptibility" $\bar{\chi}$, which we obtain by inserting $\bar{\psi}(c)$ into Eq. (2.7),

$$\bar{\chi}(c)=\chi_n, \quad c_1<c<c_n \ , \tag{3.5a}$$

$$\bar{\chi}(c)=\chi_n\left(\frac{u+3v\bar{\psi}^2}{-|\tilde{u}|+3v\bar{\psi}^2}\right), \quad c_s<c<c_1 \ . \tag{3.5b}$$

It is this quantity which turns out to enter the nonequilibrium versions of the equations of motion (2.13). Note that $\chi_n$ is *not* the limit of Eq. (3.5b) as $\bar{\psi}\to 0$. This is to be expected, since Eq. (3.5a) corresponds to a different branch of the free energy than Eq. (3.5b). From Eq. (3.5b), one is immediately led to define a spinodal point $c_\sigma$ at which $|\tilde{u}|=3v|\psi|^2$ and $\bar{\chi}^{-1}=0$. Note that $\bar{\chi}^{-1}$ is negative for $c_\sigma<c<c_1$, and that the above analysis can be repeated at every temperature in the coexistence volume.

As shown in Appendix A, it is possible to express the constrained quantities $\bar{\psi}$ and $\bar{\chi}$ entirely in terms of the measurable equilibrium values of $\psi_s(T)$, $\chi_s(T)$, $\chi_n(T)$, $c_s(T)$, and $c_n(T)$, via the parameter

$$\rho\equiv\tfrac{1}{2}(\chi_s-\chi_n)/\chi_n \ . \tag{3.6}$$

The concentrations $c_1$ and $c_\sigma$ defined above are then also expressible entirely in terms of $c_n$, $c_s$, and $\rho$. In mean-field theory $\chi_n$ is a constant, and Eqs. (2.7b) and (2.8) imply that

$$\rho=\chi_n\gamma^2/|\tilde{u}|\propto t_t^{-1}\gg 1 \ , \tag{3.7}$$

where

$$t_t\equiv|T_t-T|/T_t \ . \tag{3.8}$$

Experimentally, however, $\chi_n$ diverges at $T_t$ in $^3$He-$^4$He mixtures [see Eq. (C5)], and the parameter $\rho$ is essentially constant near $T_t$, with

$$\rho\approx 4.5 \ , \tag{3.9}$$

which is also rather large. The expressions for $\bar{\psi}$ and $\bar{\chi}$ simplify in the limit of large $\rho$, where we find

$$\bar{\chi}^2/\chi_s^2\approx(c_n-c)/(c_n-c_s) \ , \tag{3.10}$$

$$\chi_s/\bar{\chi}\approx[3(c_n-c)/(c_n-c_s)]-2 \ , \tag{3.11}$$

$$c_n-c_1=(1/4\rho)(c_n-c_s) \ , \tag{3.12}$$

$$c_n-c_\sigma\approx\tfrac{2}{3}(c_n-c_s) \ . \tag{3.13}$$

The function $\bar{\chi}$ is plotted in Fig. 4.

Our results thus far can be summarized as follows: The two-phase region of the $(T,c)$ phase diagram is divided into three wedges: an inner portion, for which $\bar{\chi}^{-1}<0$ $(c_\sigma<c<c_1)$, and two outer portions $(c_s<c<c_\sigma$ and $c_1<c<c_n)$ where $\bar{\chi}^{-1}>0$. Note from Eqs. (3.9), (3.12), and (3.13), that these three wedges should be quite asymmetrically placed. Indeed, were we to take mean-field theory literally and assume $\chi_n\approx$const near the tricritical point, Eqs. (3.9) and (3.14) would predict (using $c_n-c_s\propto|T-T_t|$) that

$$c_n-c_1\propto|T-T_t|^2 \ , \tag{3.14a}$$

in contrast to Eq. (3.15),

$$c_n-c_\sigma\propto|T-T_t| \ . \tag{3.14b}$$

We feel, however, that a more realistic estimate of the lines $c_1$ and $c_\sigma$ of Fig. 1(b) can be obtained from Eqs. (3.12) and (3.13), using the *measured* value of $\rho$ at any temperature.

To conclude this discussion of the constrained susceptibility $\bar{\chi}$, note that the above calculation can be repeated for finite wave-vector disturbances. The result, using Eq. (2.1), is

$$\bar{\chi}^{-1}(k)=\bar{\chi}^{-1}+l_0^2k^2$$
$$=\bar{\chi}^{-1}[1+(\bar{\chi}/\chi_s)k^2\xi_s^2] \ , \tag{3.15}$$

where

$$\xi_s^2=l_0^2\chi_s \tag{3.16}$$

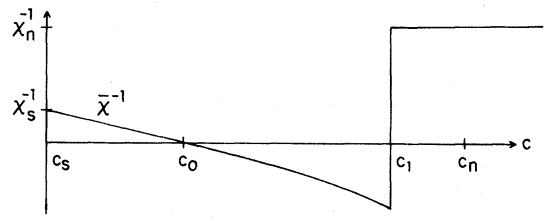


FIG. 4. Constrained susceptibility $\bar{\chi}$ as a function of concentration at fixed temperature, as given by Eq. (3.11). For clarity of the figure we have chosen $\chi_s\simeq 4\chi_n$. The spinodal region $c_\sigma<c<c_1$ has $\bar{\chi}^{-1}<0$, with $\bar{\chi}^{-1}=0$ at $c\sigma$ and a jump at $c_1$. In the present approximation we have $\bar{\chi}=\chi_n=$const, for $c>c_1$.

is the square of the concentration correlation length in the superfluid.

### B. Spinodal dynamics

The foregoing analysis of the two-phase region focused entirely on the static quantities $\bar{\psi}$ and $\bar{\chi}$. To draw further conclusions we now describe the response of the system following the rapid relaxation of $|\psi|$ to its constrained value. We shall use the remaining hydrodynamic equations, (2.13), for the conserved variables $c(x,t)$, $q(x,t)$, and $\theta(x,t)$, linearized, say, about the point $B_2$ of Fig. 3(b).

This linearization is carried out in Appendix B. Just as in the equilibrium superfluid, there are three hydrodynamic modes whenever $\bar{\psi}^2$ is nonzero, a diffusion mode[16]

$$\bar{\omega}_0 = \bar{D}_0 k^2 + O(k^4) \ , \tag{3.17}$$

and two second-sound modes

$$\bar{\omega}_\pm = \pm i\bar{u}_2 k + \tfrac{1}{2}\bar{D}_2 k^2 + O(k^3) \ . \tag{3.18}$$

The full expressions for $\bar{D}_0$, $\bar{D}_2$, and $\bar{u}_2$ in terms of the model parameters are given in Eqs. (B4)–(B13). It is convenient at this point to note that $\bar{D}_0$ and $\bar{u}_2$ may be written

$$\bar{D}_0 = \kappa_{\rm eff} g_2^2 / g_1^2 \bar{\chi}(1+\Phi) \ , \tag{3.19}$$

$$\bar{u}_2^2 = \bar{\psi}^2 g_1^2 (1+\Phi)/C \ , \tag{3.20}$$

where $\bar{\chi}$ and $\bar{\psi}^2$ are the constrained quantities discussed in Sec. III A. The parameters, $\kappa_{\rm eff}$, $g_1$, $g_2$, and $c$ remain positive and finite near the tricritical point in the mean-field approximation, while $\Phi$ vanishes as $T \to T_t^-$, and will be neglected here.

The calculation of the nonequilibrium correlation functions outlined in Appendix B leads to the result quoted in Eq. (1.8), namely,

$$S(k,t) = a_1 e^{-2\bar{D}_0 k^2 t} + a_2 e^{-(\bar{D}_0+\bar{D}_2)k^2 t}\cos\bar{u}_2 kt + a_3 e^{-2\bar{D}_2 k^2 t}\cos 2\bar{u}_2 kt + a_0 \ . \tag{3.21}$$

The analysis of Appendix C shows that near the tricritical point we may write

$$\bar{D}_0(k) \approx D_{0s}(\chi_s/\bar{\chi} + k^2\xi_s^2) \ , \tag{3.22}$$

$$\bar{u}_2^2 \approx u_{2s}^2(\bar{\psi}^2/\psi_s^2) \ , \tag{3.23}$$

$$\bar{D}_2 \approx D_{2s} \ , \tag{3.24}$$

where $D_{0s}$, $u_{2s}$, $\xi_s$, and $D_{2s}$ are the corresponding equilibrium quantities on the superfluid side of the phase-separation curve at the given quench temperature.

Equation (3.21) predicts unstable growth of concentration fluctuations whenever $\bar{D}_0 < 0$, which according to Eq. (3.22) occurs when $\bar{\chi}^{-1} < 0$, i.e., for $c_\sigma < c < c_1$. The wave vector of maximum growth can be estimated in the way discussed in the Introduction and turns out to be

$$k_m = \xi_s^{-1}(\tfrac{1}{2}|\chi_s/\bar{\chi}|)^{1/2} \ . \tag{3.25}$$

The corresponding frequency is

$$|\bar{\omega}_{0m}| = \tfrac{1}{4} D_{0s} k_m^2 |\chi_s/\bar{\chi}| = \tfrac{1}{8} D_{0s}\xi_s^{-2}(\chi_s^2/\bar{\chi}^2) \ . \tag{3.26}$$

The quantities $D_{0s}$ and $\xi_s$ have been measured by light scattering in the superfluid phase, and the results near $T_t$ are [Eqs. (C10) and (C11)]

$$D_{0s} = 2.5\times 10^{-4} t_t \ {\rm cm^2/sec} \ , \tag{3.27}$$

$$\xi_s = 1.3 t_t^{-1} \ \text{Å} \ , \tag{3.28}$$

leading to

$$|\bar{\omega}_{0m}| = 1.8\times 10^{11} t_t^2 (\chi_s/\bar{\chi})^2 \ {\rm sec^{-1}} \ , \tag{3.29}$$

$$k_m = 0.54 t_t |\chi_s/\bar{\chi}|^{1/2} \ \text{Å}^{-1} \ . \tag{3.30}$$

In the metastable regions of Fig. 1(b) (i.e., $c_1 < c < c_n$ or $c_s < c < c_\sigma$, $\bar{\chi}^{-1} > 0$), the linear analysis predicts a stable correlation function, i.e., $\bar{\omega}_0 > 0$. Phase separation presumably proceeds via a nucleation mechanism in this case.[7]

According to Eq. (3.23) the second-sound frequency $\bar{u}_2 k$ remains real, its magnitude at $k = k_m$ being of order

$$\bar{\omega}_{2m} \approx u_{2s}\xi_s^{-1}(\chi_s\bar{\psi}^2/2|\bar{\chi}|\psi_s^2)^{1/2} \ . \tag{3.31}$$

Equation (3.21) predicts that in addition to the instability represented by the first term, there will be an oscillating component, proportional to $a_2$, which is a "flickering" of the instability, caused by coupling of diffusion and second sound. This feature can only be seen if the exponential factor leads to growth, i.e., if $\bar{D}_0 + \bar{D}_2 < 0$. Inserting the estimates (3.22) and (3.24) we need

$$D_{0s} \gtrsim 2D_{2s} \ , \tag{3.32}$$

since $|\chi_s/\bar{\chi}| < 2$. The second-sound damping $D_{2s}$ has been measured, but from scaling arguments[17] it is expected to diverge near $T_t$, so that in view of Eq. (3.27) the inequality (3.32) is not expected to hold in the critical region. It appears doubtful, but not impossible, that a region of temperatures can be found below $T_t$ where Eq. (3.32) will hold, and where the "flickering" might be observable.

Let us discuss briefly the effect of the coefficient

$$\Phi \equiv g_2^2 C/g_1^2\bar{\chi} \ , \tag{3.33}$$

which we neglected in Eqs. (3.19) and (3.20), since $\Phi$ vanishes at $T_t$. According to the numerical estimates of Appendix B, however, the quantity $1+\Phi$ is predicted to become negative in a region of the phase

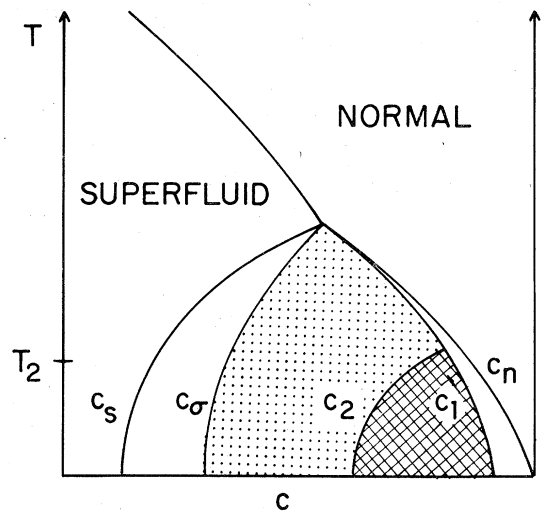


FIG. 5. Two-phase region in $^3$He-$^4$He mixtures with account taken of the term $\Phi$ of Eqs. (B7)–(B9). In the cross-hatched region $c_2 < c < c_1$ appearing below $T_2$, the second-sound mode becomes unstable.

diagram appearing below some temperature $T_2$, which we estimate to be 0.55 °K [see Fig. 5]. In this region, Eqs. (3.19) and (3.20) imply that second sound becomes unstable, while the diffusion mode is stabilized. Needless to say, the relevance of our model to experiment becomes more questionable as one goes further below $T_t$, but it would be interesting to see if any of the anomalies associated with this effect can be detected experimentally. Further discussion of these points is included in Appendix B.

Another anomaly, which is in principle possible at lower temperatures, is associated with a change of sign of the coefficient $u$, which is positive near $T_t$. For $u < 0$ our model predicts different values of $\bar{\psi}$ depending on whether the quench is initiated in the superfluid or normal one-phase regions. From Eq. (2.8) we see that $u < 0$ for $\chi_s \leq 3\chi_n$, which we estimate to happen below $T \approx 0.6$ K.

*Note added in proof:* It has recently come to our attention that spinodal decomposition in *alloy* systems has been treated by S. M. Allen and J. W. Cahn, Acta Metall. 23, 1017 (1975); 27, 1085 (1979); and to be published.

## ACKNOWLEDGMENTS

We have benefited from discussions with H. Meyer, G. Ahlers, and B. I. Halperin, and are particularly indebted to P. Leiderer for stimulating our interest in this problem. One of us (P.C.H.) was a visitor of the Harvard Physics Department during a portion of this work. D.R.N. would like to acknowledge support from a Junior Fellowship, Harvard Society of Fellows, and the hospitality of Bell Laboratories, where this collaboration was initiated. Work at Harvard was supported in part by the NSF under Grant No. DMR 77-10210.

## APPENDIX A: CONSTRAINED SUPERFLUID ORDER PARAMETER $\bar{\psi}$ AND CONCENTRATION SUSCEPTIBILITY $\bar{\chi}$

In this Appendix we calculate $\bar{\psi}$ and $\bar{\chi}$ and relate them to measurable quantities. The initial relaxation of the magnitude of $\psi$ is determined by the first term on the right-hand side of Eq. (2.9a), since the other terms couple to the phase of $\psi$, as does the term in $q^2$ in Eq. (2.10). We may thus write

$$\frac{\partial|\psi|}{\partial t} = -\Gamma\frac{\delta\mathcal{F}}{\delta|\psi|} = -2\Gamma|\psi|[c-\bar{c}(|\psi|)] \ , \quad \text{(A1)}$$

$$\bar{c}(|\psi|) \equiv -[(r/2\gamma)+(2u/\gamma)|\psi|^2+(3v/\gamma)|\psi|^4] \ , \quad \text{(A2)}$$

as in Eq. (3.2). It follows that $|\psi|$ relaxes rapidly to a value $\bar{\psi}$ obtained from the initial concentration $c$ and temperature $r < 0$ by inverting the relation

$$c = \bar{c}(\bar{\psi}) \ . \quad \text{(A3)}$$

This yields

$$3v\bar{\psi}^2 = -u + [u^2 + 3\gamma v(c_n - c) - \tfrac{3}{4}\tilde{u}^2]^{1/2} \ , \quad \text{(A4)}$$

where we have used Eqs. (2.3b) and (2.4) and the relation $\tilde{u}^2 = 2\tilde{r}v$ valid in the two-phase region, to eliminate $r$ and $\tilde{r}$. The constrained susceptibility $\bar{\chi}$ is then obtained by inserting Eq. (A4) into Eq. (2.7a), as in Eq. (3.5). We may now express $\psi$ and $\bar{\chi}$ in terms of measurable quantities by using Eqs. (A4), (2.5), (2.6), (2.8), and (3.6), to write

$$\frac{\bar{\psi}^2}{\psi_s^2} = \frac{2}{3}(\rho-1)\left\{\left[1+\frac{3\rho}{(\rho-1)^2}\left(\frac{c_n-c}{c_s-c}-\frac{1}{4\rho}\right)\right]^{1/2}-1\right\} \ , \quad \text{(A5)}$$

$$\frac{\chi_s}{\bar{\chi}} = (1+2\rho)\left(\frac{3}{2}\frac{\bar{\psi}^2}{\psi_s^2}-1\right)\Big/\left(\frac{3}{2}\frac{\bar{\psi}^2}{\psi_s^2}+\rho-1\right) \ . \quad \text{(A6)}$$

Equation (A5) implies that $\bar{\psi}$ vanishes at a concentration $c = c_1$ such that

$$(c_n - c_1)/(c_n - c_s) = 1/4\rho \ , \quad \text{(A7)}$$

which can be shown to agree with Eq. (3.4b). The spinodal line $c_\sigma$ at which $\bar{\chi}^{-1}$ vanishes is obtained in terms of $c_n$, $c_s$, and $\rho$ from Eqs. (A5) and (A6). In the limit of large $\rho$ one easily finds the expressions in Eqs. (3.10)–(3.13).

## APPENDIX B: SOLUTION OF THE LINEARIZED LANGEVIN EQUATIONS

In this Appendix we treat the spinodal decomposition which occurs after the initial rapid relaxation of

$|\psi|$ to $\bar{\psi}$ and $\chi$ to $\bar{\chi}$. We use the hydrodynamic model (2.9) in its linearized form shown in Eq. (2.13), but with $\bar{\psi}$ and $\bar{\chi}$ written in place of $\psi$ and $\chi$. Let us rewrite Eqs. (2.13) as

$$\frac{\partial \vec{u}}{\partial t} = -\underline{\Omega} \cdot \vec{u} + \vec{\eta} \ , \tag{B1}$$

in terms of the vectors $\vec{u}(t) = (\theta, q, c)$ and $\vec{\eta} = (\eta_\theta, \eta_q, \eta_c)$ (we are suppressing the variables $k$ and $t$). The matrix $\underline{\Omega}$ is given by

$$\underline{\Omega} = \begin{pmatrix} \Gamma k^2 & -g_1 C^{-1} & -g_2 \bar{\chi}^{-1} \\ g_1 \bar{\psi}^2 k^2 & K C^{-1} k^2 & L \bar{\chi}^{-1} k^2 \\ g_2 \bar{\psi}^2 k^2 & L C^{-1} k^2 & \lambda \bar{\chi}^{-1} k^2 \end{pmatrix} \tag{B2}$$

and has eigenvalues $\omega$ satisfying the equation

$$(\omega - \Gamma k^2)(\omega - D_+ k^2)(\omega - D_- k^2) + \omega \bar{u}_2^2 k^2 - \bar{D}_0 \bar{u}_2^2 k^4 = 0 \ , \tag{B3}$$

with

$$D_+ + D_- = \lambda \bar{\chi}^{-1} + K C^{-1} \ , \tag{B4}$$

$$D_+ D_- = \lambda (K - L^2/\lambda)/\bar{\chi} C \equiv \lambda \kappa / \bar{\chi} C \ , \tag{B5}$$

$$\bar{D}_0 = \frac{\lambda g_1^2 + K g_2^2 - 2 L g_1 g_2}{g_1^2 \bar{\chi} + g_2^2 C} \ , \tag{B6}$$

$$= g_2^2 \kappa_{\text{eff}} / g_1^2 (1 + \Phi) \bar{\chi} \ , \tag{B7}$$

$$\kappa_{\text{eff}} \equiv \kappa + \lambda (g_1/g_2 - L/\lambda)^2 \ , \tag{B8}$$

$$\Phi \equiv g_2^2 C / g_1^2 \bar{\chi} \ , \tag{B9}$$

$$\bar{u}_2^2 = \bar{\psi}^2 g_1^2 C^{-1} (1 + \Phi) \ . \tag{B10}$$

The solutions of Eq. (B3) to lowest order in $k$ are[16]

$$\bar{\omega}_0 = \bar{D}_0 k^2 + O(k^4) \ , \tag{B11}$$

$$\bar{\omega}_\pm = \pm i \bar{u}_2 k + \tfrac{1}{2} \bar{D}_2 k^2 + O(k^3) \ , \tag{B12}$$

$$\bar{D}_2 = D_+ + D_- + \Gamma - \bar{D}_0 \ . \tag{B13}$$

When the system is in equilibrium in the one-phase region, Eqs. (B1) may be used to calculate the time-dependent correlation or response functions, in the usual way.[13] The modes (B11)–(B15) appear as poles, with $\bar{\chi}$, $\bar{\psi}$, and $\bar{u}_2$ replaced by the usual equilibrium values $\chi_s$, $\psi_s$, $u_{2s}$. Equations (B11)–(B13) for the diffusion and second-sound modes in the superfluid phase correspond with those of Griffin[13] and Khalatnikoy[12] (with the transcription of notation defined in Table I). Equation (B12) also reduces to the usual second-sound mode for pure $^4$He ($g_2 = 0$).[15] In the normal phase ($\psi = 0$), Eq. (2.13a) does not hold, since it was obtained from Eq. (2.9a) by dividing by $|\psi|^2$. The hydrodynamics then involves the two coupled modes $q$ and $c$, and diagonalization of the appropriate $2 \times 2$ matrix yields the modes[18]

TABLE I. Comparison of parameters of Ref. 11 with those of Refs. 12 and 13.

| Khalatnikov-Griffin | Present paper and Ref. 11 |
|---|---|
| $k_B T \bar{\sigma}/\hbar$ | $g_1$ |
| $k_B T c/\hbar$ | $g_2$ |
| $(TR)^{-1} \partial \tilde{Z}/\partial c$ | $\chi^{-1}$ |
| $R^{-1} C_{p,c}$ | $C$ |
| $\kappa/\rho^{a}$ | $\kappa = K - L^2/\lambda$ |
| $k_T$ | $\chi L/\lambda$ |
| $D$ | $\lambda/\chi$ |
| $h^2 \rho_s/\rho_n m k_B T$ | $\psi_s^2$ |
| $\rho_s \zeta_3$ | $\Gamma$ |

[a]Griffin (see Ref. 13) uses $K$ for the quantity denoted $\kappa$ by Khalatnikov (Ref. 12). $R$ is the gas constant.

$$\omega_1 = D_+ k^2 \ , \tag{B14}$$

$$\omega_2 = D_- k^2 \ . \tag{B15}$$

In the case of a rapid quench, we can calculate the correlation functions

$$S_{\alpha\beta}(t) = \langle u_\alpha(t) u_\beta(t) \rangle \ , \tag{B16}$$

solving the matrix Langevin equation (B1). Let $\underline{U}$ be the matrix which diagonalizes $\underline{\Omega}$

$$(\underline{U} \underline{\Omega} \underline{U}^{-1})_{\alpha\beta} = \omega_\alpha \delta_{\alpha\beta} \ . \tag{B17}$$

If we define

$$\vec{v} = \underline{U} \cdot \vec{u} \ , \tag{B18}$$

$$\vec{\zeta} = \underline{U} \cdot \vec{\eta} \ , \tag{B19}$$

then

$$v_\alpha = -\omega_\alpha v_\alpha + \zeta_\alpha \ , \tag{B20}$$

where the $\omega_\alpha$ are given by Eqs. (B11) and (B12). The solution of Eq. (B20) is analogous to Eq. (1.5), and we find

$$\langle v_\alpha(t) v_\beta(t) \rangle = e^{-(\omega_\alpha + \omega_\beta)t} \left[ \langle v_\alpha(0) v_\beta(0) \rangle - \frac{2\tilde{\Gamma}_{\alpha\beta}}{\omega_\alpha + \omega_\beta} \right] + \frac{2\tilde{\Gamma}_{\alpha\beta}}{\omega_\alpha + \omega_\beta} \ , \tag{B21}$$

where

$$\langle \zeta_\alpha(1) \zeta\beta(1') \rangle \equiv 2\tilde{\Gamma}_{\alpha\beta} \delta(1 - 1') = U_{\alpha\gamma} \langle \eta_\gamma(1) \eta_\delta(1') \rangle U_{\delta\beta} \equiv 2\delta(1 - 1') U_{\alpha\gamma} \Gamma_{\gamma\delta} U_{\delta\beta} \ . \tag{B22}$$

The physical correlation functions are given by

$$S_{\alpha\beta}(t) = \langle u_\alpha(t) u_\beta(t) \rangle = u^{-1}_{\alpha\gamma} U_{\gamma\gamma'} U^{-1}_{\beta\delta} U_{\delta\delta'} e^{-(\omega_\gamma + \omega_\delta)t} \times \left[ S_{\gamma'\delta'}(0) + \frac{2\Gamma_{\gamma'\delta'}}{\omega_\gamma + \omega_\delta} \left( e^{(\omega_\gamma + \omega_\delta)t} - 1 \right) \right] . \tag{B23}$$

Thus each correlation function is made up of terms proportional to $\exp(-2\bar{\omega}_0 t)$, $\mathrm{Re}\exp[-(\bar{\omega}_0 + \bar{\omega}_+)t]$, and $\mathrm{Re}\exp(-2\bar{\omega}_+ t)$, with complicated coefficients depending on the elements of the matrix $\underline{U}$. This is the result indicated in Eq. (3.21). The frequencies $\bar{\omega}_0$ and $\bar{\omega}_+$ can be related to the corresponding diffusion and second-sound modes $\omega_{0s}$, $\omega_{+s}$ at the same temperatures in the equilibrium superfluid phase. Since the quantity $\Phi$ in Eqs. (B7) and (B10) vanishes near the tricritical point, we shall first neglect its contribution. Then $\bar{D}_0$ and $\bar{u}_2$ are given by

$$\bar{D}_0 \simeq (\chi_s/\bar{\chi}) D_{0s} , \tag{B24}$$

$$\bar{u}_2^2 \simeq (\bar{\chi}^2/\chi_s^2) u_{2s}^2 . \tag{B25}$$

At finite $k$ we replace $\bar{\chi}^{-1}$ by $\bar{\chi}^{-1} + l_0^2 k^2$ [Eq. (3.15)], and we have

$$\bar{\omega}_0(k) = \chi_s/(\bar{\chi}^{-1} + l_0^2 k^2) D_{0s} = D_{0s}(\chi_s/\bar{\chi} + \xi_s^2 k^2) , \tag{B26}$$

$$\bar{\omega}_+(k) = u_{2s}(\bar{\chi}^2/\chi_s^2) k . \tag{B27}$$

Let us now discuss briefly the effect of $\Phi$ in Eqs. (B7) and (B10). According to the estimates of Appendix C, Eq. (C8), we have

$$\Phi_s \equiv g_2^2 C/g_1^2 \chi_s = 1.2 t_t \tag{B28}$$

and since $|\chi_s/\bar{\chi}| < 2 + (\rho - 1)^{-1} \approx 2.3$, it is legitimate to set $1 + \Phi \simeq 1$ near the tricritical point ($t_t \to 0$). It is nevertheless interesting to explore the regions of $T$ and $c$ where the factor $1 + \Phi$ can vanish, since the dynamical equations are then drastically modified. Indeed, suppose that for some temperature we have

$$\Phi_s \geq -\left( \frac{\bar{\chi}(c_1)}{\chi_s(c_1)} \right) = [2 + (\rho - 1)^{-1}]^{-1}; \tag{B29}$$

then there is an interval $c_2 < c < c_1$, in which $1 + \Phi < 0$, with $c_2$ defined by

$$\Phi_s = -\bar{\chi}(c_2)/\chi_s(c_2) . \tag{B30}$$

In that case the model predicts that $\bar{D}_0$ is positive for $c_2 < c < c_n$, *diverges* at $c = c_2$, and is negative for $c_\sigma < c < c_2$. The velocity $\bar{u}_2$ is imaginary for $c_2 < c < c_1$, i.e., second sound is also an unstable mode,[16]

$$\bar{\omega}_\pm = \pm |\bar{u}_2| k + \tfrac{1}{2} \bar{D}_2 k^2 . \tag{B31}$$

Moreover, Eq. (B13) implies that the second-sound damping coefficient $\bar{D}_2$ becomes negative for $c \gtrsim c_2$, since $\bar{D}_0$ is large and positive. The behavior of the correlation functions in the region $c_2 < c < c_1$ shown in Fig. 5, will be quite anomalous, although as mentioned earlier it is not clear how far below $T_t$ our model can be trusted. From Eqs. (B29) and (B30) and the estimates given in Appendix C we find that $c_2$ first appears at $t_t \simeq 0.36$, i.e., below $T = 0.55$ (see Fig. 5). A more accurate estimate of $\Phi$ may be obtained by using Eqs. (B9), (A5), and (A6). In this way the frequencies in Eqs. (B11) and (B12) may be expressed throughout the two-phase region in terms of measurable equilibrium properties.

## APPENDIX C: EXPERIMENTAL ESTIMATES OF PARAMETERS

In the model defined in Eq. (3.1) we have chosen units such that $\mathcal{F}$ and $c$ are dimensionless, i.e., $\mathcal{F}$ represents the free energy per particle divided by $k_B T$. It follows that $\chi_n$ is dimensionless and $|\psi|^2$ has units of (length)$^2$. For the dynamic model, Eqs. (2.9)–(2.11), we also take $W$, $q$, and $C$ to be dimensionless, $g_1$ and $g_2$ to have dimensions of frequency, and $L$, $\kappa$, $\lambda$, $\Gamma$, with dimensions of a diffusion constant ($l^2/t$). With these conventions, we then establish the correspondence with the parameters of Khalatnikov,[12] shown in Table I. The quantity $\bar{\sigma} = \sigma - c\,\partial\sigma/\partial c$ in the left-hand column is dimensionless, with $\sigma \equiv S/R$ equal to the entropy per particle, in units of $k_B$. The susceptibility $\partial\tilde{Z}/\partial c$ is in joules/mole, and the specific heat $C_{p,c}$ is in joules/mole K, thus making $\chi$ and $C$ dimensionless.

The parameters entering Eqs. (3.22) and (3.24) are related to quantities which are in principle measurable, in either the superfluid or the normal phase, for arbitrary temperatures. Many of these, however, are only known approximately, and typically only near the tricritical point. We have often approximated regular quantities by their value at $T_t$, and we have estimated from various sources those quantities which were not explicitly published. Clearly, more accurate determinations of parameters in the one-phase regions would help to refine our estimates for the two-phase properties.

The important quantities we need are[8,9,19,20]

$$c = c_t = 0.67 , \tag{C1}$$

$$\bar{\sigma} = 0.52 , \tag{C2}$$

and[20]

$$\left( \frac{\partial \tilde{Z}}{\partial c} \right)_{c = c_s} = 6.0 t_t \text{ joules/mole} . \tag{C3}$$

This implies

$$\chi_s^{-1} = 0.83 t_t \ , \tag{C4}$$

$$\chi_n^{-1} = 8.3 t_t \ , \tag{C5}$$

$$C \approx C_{p,c}/R = 0.92 \ , \tag{C6}$$

$$g_1/g_2 = \bar{\sigma}/c = 0.8 \ , \tag{C7}$$

$$\Phi_s \equiv g_2^2 C/g_1^2 \chi_s = 1.2 t_t \ . \tag{C8}$$

If the measured thermal conductivity is $\tilde{\kappa}_{\text{eff}}$ we have[19]

$$\kappa_{\text{eff}} = \bar{\kappa}_{\text{eff}}/\rho R = 1.9 \times 10^{-4} \text{ cm}^2/\text{sec} \ , \tag{C9}$$

so that[9]

$$D_{0s} = \frac{\kappa_{\text{eff}} g_2^2}{g_1^2 \chi_s (1+\Phi_s)} = \frac{2.5 \times 10^{-4} t_t}{1+1.2 t_t} \text{ cm}^2/\text{sec} \ . \tag{C10}$$

Finally, the measured correlation length near $t_t$ is[8]

$$\xi_s = 1.3 t_t^{-1} \text{ Å} \ . \tag{C11}$$


[1]See J. S. Langer, in *Fluctuations, Instabilities and Phase Transitions,* edited by T. Riste (Plenum, New York, 1975), and references therein.

[2]W. I. Goldberg and J. S. Huang, in *Fluctuations, Instabilities and Phase Transitions,* edited by T. Riste (Plenum, New York, 1975), and references therein; W. I. Goldburg, C. H. Shaw, J. S. Huang, and M. S. Pilant, J. Chem. Phys. 68, 484 (1978); N. C. Wong and C. M. Knobler, J. Chem. Phys. 69, 725 (1978).

[3]See, e.g., J. S. Langer, M. Bar-on, and H. Miller, Phys. Rev. A 11, 1417 (1975); K. Binder, Phys. Rev. B 15, 4425 (1977); K. Kawasaki and T. Ohta, Prog. Theor. Phys. (Japan) 59, 362 (1978); and E. D. Siggia (unpublished).

[4]J. W. Cahn, Acta Metall. 9, 795 (1961); 10, 179 (1962).

[5]J. E. Hilliard, in *Phase Transformations,* edited by H. I. Aronson (American Society for Metals, Cleveland, 1970).

[6]H. E. Cook, Acta Metall. 18, 297 (1970).

[7]See also I. M. Lifshitz, V. N. Polesskii, and V. A. Khokhlov, Zh. Eksp. Teor. Fiz. 74, 268 (1978) [Sov. Phys. JETP 47, 137 (1978)].

[8]P. Leiderer, D. R. Watts, and W. W. Webb, Phys. Rev. Lett. 33, 483 (1974).

[9]P. Leiderer, D. R. Nelson, D. R. Watts, and W. W. Webb, Phys. Rev. Lett. 34, 1080 (1975).

[10]P. Leiderer (private communication).

[11]E. D. Siggia and D. R. Nelson, Phys. Rev. B 15, 1427 (1977).

[12]I. M. Khalatnikov, *An Introduction to the Theory of Superfluidity* (Benjamin, New York, 1965), Chap. 24; Zh. Eksp. Teor. Fiz. 23, 265 (1952).

[13]A. Griffin, Can. J. Phys. 47, 429 (1969).

[14]See, e.g., R. Bausch, Z. Phys. 254, 81 (1972).

[15]B. I. Halperin, P. C. Hohenberg, and E. D. Siggia, Phys. Rev. B 13, 1299 (1976).

[16]We adopt a convention such that the time evolution of a hydrodynamic excitation is $e^{-\omega t}$. Thus, a positive real frequency $\omega$ signifies a damped mode, and imaginary frequencies oscillatory modes.

[17]B. I. Halperin and P. C. Hohenberg, Phys. Rev. 177, 952 (1969).

[18]L. D. Landau and E. M. Lifshitz, *Fluid Mechanics,* (Addison-Wesley, Reading, Mass., 1959), Chap. VI.

[19]G. Ahlers, in *The Physics of Liquid and Solid Helium, Part I,* edited by K. H. Bennemann and J. B. Ketterson (Wiley, New York, 1976), p. 85; and private communications.

[20]G. Goellner, R. Behringer, and H. Meyer, J. Low Temp. Phys. 13, 113 (1973).